Spatial association between COVID-19 incidence rate and nighttime light index

Amornrat Luenam,[1] Nattapong Puttanapong[2]

[1]*Faculty of Public and Environmental Health, Huachiew Chalermprakiet University, Samut Prakan;*
[2]*Faculty of Economics, Thammasat University, Bangkok, Thailand*

Abstract

This study statistically identified the localised association between socioeconomic conditions and the coronavirus disease 2019 (COVID-19) incidence rate in Thailand on the basis of the 1,727,336 confirmed cases reported nationwide during the first major wave of the pandemic (March-May 2020) and the second one (July 2021-September 2021). The nighttime light (NTL) index, formulated using satellite imagery, was used as a provincial proxy of monthly socioeconomic conditions. Local indicators of spatial association statistics were applied to identify the localised bivariate association between COVID-19 incidence rate and the year-on-year change of NTL index. A statistically significant negative association was observed between the COVID-19 incidence rate and the NTL index in some central and southern provinces in both major pandemic waves. Regression analyses were also conducted using the spatial lag model (SLM) and the spatial error model (SEM). The obtained slope coefficient, for both major waves of the pandemic, revealed a statistically significant negative association between the year-on-year change of NTL index and COVID-19 incidence rate (SLM: coefficient= −0.0078 and −0.0064 with P<0.001 and 0.056, respectively; and SEM: coefficient= −0.0086 and −0.0083 with P=0.067 and 0.056, respectively). All of the obtained results confirmed the negative association between the COVID-19 pandemic and socioeconomic activity revealing the future extensive applications of satellite imagery as an alternative data source for the timely monitoring of the multidimensional impacts of the pandemic.

Introduction

The coronavirus 2019 (COVID-19) pandemic emerged in Wuhan, Hubei Province, China, in December 2019 and increased in January 2020 (Grainger *et al.,* 2021). In February 2022, the global number of confirmed cases has exceeded 408 million (WHO, 2022), and the total number of deaths is more than 5.8 million (WHO, 2022). Many countries have experienced multiple waves of coronavirus outbreaks. Empirical data show that the characteristics of the disease varied between waves during the 2020 pandemic (Iftimie *et al.,* 2021).

The first COVID-19 infected case in Thailand was confirmed on January 13, 2020, in a Chinese tourist hospitalised in Bangkok. This case is the first globally reported outside China (WHO, 2020). On January 30, 2020, Thailand's Ministry of Public Health (MoPH) publicly announced the first case of local transmission. The newly infected cases increased rapidly in March 2020, spreading from the major clusters of boxing stadiums and entertainment venues and initiating the first major wave of the pandemic (ADB, 2021).

During the first major wave (March-May 2020), the number of new COVID-19 cases increased to approximately 3040, and nearly 60 deaths were recorded. A second major wave occurred in July-September 2021, during which the number of daily new cases increased to more than 20,000, and the daily recorded deaths rose to more than 100 (WHO, 2021). Consequently, the Thai government imposed lockdown measures and required most of the provinces in Thailand to implement strict policies to limit non-essential activities, transportation, and production. Most people volunteered to stay at home, and the practice of self-isolation

played an essential role in curbing the spread. However, the effects of COVID-19 are multidimensional. Not only have they stretched health system responses, but they already exposed vulnerabilities in the economy and society (World Bank, 2021; Kunno *et al.,* 2021).

In October 2021, the spread of COVID-19 was considered substantially controlled in Thailand. However, the pandemic situation is still severe in other parts of the world. Most studies have investigated how control measures affect the outbreak (Kraemer *et al.,* 2020). Globally, only a limited number of studies have fully utilised the capability of data and analytical methods to examine the characteristics and consequences of the COVID-19 pandemic and the containment measures (Bergquist and Rinaldi, 2020; Ahasan and Hossain, 2021; Fatima *et al.*, 2021).

With the evolution of continuously increasing public accessibility, remote sensing data and spatial analysis are widely used in studies on natural disasters and the spread of epidemics (Cao *et al.,* 2010; Xu *et al.,* 2013; Liu *et al.,* 2019). Particularly, nighttime light (NTL) shown on satellite imagery can identify the boundary of cities and quantitatively indicate the density of economic activities and socioeconomic status (Liu *et al.,* 2020). NTL has been commonly used in social and epidemiological studies as an approximate proxy for urban density and economic activity in various places, particularly in Thailand (Luenam and Puttanapong, 2020; Puttanapong *et al.*, 2020; Sangkasem and Puttanapong, 2021). Thus, in the case of the COVID-19 pandemic, the density of NTL can potentially reflect the collective reaction to the lockdown and quarantine policies.

By implementing geographic information systems (GISs) and spatial analysis methods, epidemiological studies have indicated that COVID-19 has spread in many areas with different spatial patterns (Bergquist and Rinaldi, 2020; Kolak *et al.,* 2021; Kunno *et al.,* 2021). Additionally, for multivariate association verification and predictive analyses, the spatial lag model (SLM) and the spatial error model (SEM) have been applied to the case of the COVID-19 pandemic (Sun *et al.,* 2020). However, in the case of Thailand, no COVID-19 pandemic study has used remote sensing data and spatial analysis tools.

To fill this research gap, this study examined the spatial association between COVID-19 incidence rates and socioeconomic conditions in Thailand during the two major waves of the pandemic. In addition, this study quantitatively investigated the influence of spatial spillover and developed prediction models. The obtained outcomes can provide effective solutions for developing a timely monitoring framework for COVID-19 outbreaks and future pandemics.

Materials and methods

Study area and season

This study focused on Thailand, an upper-middle-income country with an area of 514,000 km². The country comprises 511,770 km² of land and 2230 km² of water. The geographically administrative hierarchy includes 77 provinces, 878 districts (*amphoes*), 7225 sub-districts (*tambons*) and 74,965 villages (*moobans*). Located in a tropical zone, it has three seasons: winter from November to February, summer from March to May and rainy season from June to October. Figure 1 illustrates the administrative boundary and classification of the regions.
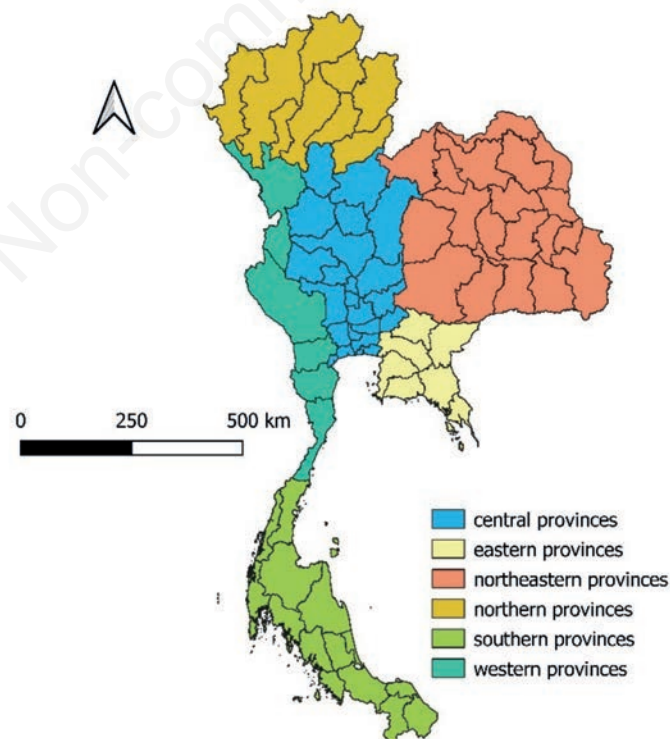
Figure 1. Regional and provincial map of Thailand.

Data sources

This cross-sectional study used COVID-19 cases from January 2020 to October 2021 as reported by the Centre of Epidemiological Information, Bureau of Epidemiology, MoPH. The data included the number of cases for all 77 provinces, with a total of 1,727,336 confirmed cases distributed over the study period. The data are publicly available at the website of MoPH's Department of Disease Control (https://covid19.ddc.moph.go.th/). In this study, the monthly COVID-19 incidence rates were computed as a ratio of confirmed cases per 100,000 population.

The NTL data of Thailand from 2020 to 2021 were acquired from the visible infrared imaging radiometer suite (VIIRS)'s day-night band global stable light imagery at a spatial resolution of 375 m^2/pixel. All NTL light data come from the joint NASA/NOAA Suomi National Polar-orbiting Partnership and are publicly available (NOAA, 2019). NTL was averaged to compute the monthly index at the provincial level, enabling the data to match the spatiotemporal resolution of the COVID-19 cases.

Analysis by the local indicator of spatial association

COVID-19 patterns were determined based on the localised detection of prevalent spatial patterns. For an exploratory spatial data analysis, QGIS version 3.8.3 (Steiniger and Hunter, 2013) and GeoDa version 1.20.0.8 (website) were used to determine the measure of spatial autocorrelation local indicators of spatial association (LISA) analysis (Anselin *et al.,* 2006). QGIS was applied to integrate all data before being transferred to GeoDa for analysis.

The spatial autocorrelation statistic (Moran's *I*) is one of the main methods for computing the degree of spatial correlation (Moran, 1950). The following equation denotes the mathematical specification of Moran's *I* test.

$$\text{Moran's } I = \frac{N \sum_i \sum_j w_{ij}(X_i - \bar{X})(X_j - \bar{X})}{\sum_i \sum_j w_{ij} \sum_i (X_j - \bar{X})^2}, \qquad (1)$$

where X_i is the variable of interest, N the number of spatial units indexed by i and j, W_{ij} the spatial weight matrix, $X_i - \bar{X}$ the deviation of X_i from its mean, and $X_j - \bar{X}$ the deviation of X_j from its mean.

The computed value indicates the correlation between X located in area i and its neighbours geographically specified by the spatial weight matrix (W_{ij}).

Moran's *I* has a limitation in identifying the location of correlation. Hence, local Moran *I* or LISA was developed by extending the mathematical fundamental of Moran's *I*. Its mathematical representation is as follows:

$$\text{Local Moran } I_i = \frac{(X_i - \bar{X}) \sum_j w_{ij}(X_j - \bar{X})}{s_i^2}, \qquad (2)$$

where $S_i^2 = \frac{\sum_j (X_j - \bar{X})^2}{(N-1)}$, W_{ij} is the spatial weight matrix, and N the number of spatial units.

The obtained output is the statistics of Moran's *I* at each loca-tion *i*, which specifies the correlation between the value of *X* in area *i* and the weighted average of its neighbours. In particular, the cluster maps obtained from LISA have four cluster categories: High-High, Low-Low, Low-High, High-Low and one pattern indicating randomness (Anselin, 2003). The statistically significant spatial correlations areas either indicate a positive bivariate association with high incidence (High-High), or a positive association of low incidence (Low-Low), while Low-High and High-Low are not the outliers. Conventionally, the COVID-19 pandemic reduces economic and social activity. Therefore, we expected areas characterised by localised negative correlation to be detected in this study.

Regression analysis

The relation between the NTL index and COVID-19 incidence rate in 77 provinces was examined with the regression models (*i.e.* SLM and SEM) by using GeoDa version 1.20.0.8 (Anselin *et al.,* 2006). Natural log transformation was used to linearise the variations in all variables. A P-value <0.10 was regarded as a criterion of statistical significance. All statistical tests were two-sided. Equations 3 and 4 shown below mathematically represent the specifications of SLM and SEM, respectively.

The mathematical specification of SLM is:

$$\Delta logNTL_i = \beta_0 + \beta_1 logCOVID19_i + \rho W_{ij} \Delta logNTL_j + \varepsilon_i, \qquad (3)$$

where $\Delta logNTL_i$ is the dependent variable (the year-on-year change in the logarithm-transformed NTL index), $logCOVID19_i$ the independent variable (the logarithm of COVID-19 incidence rate), i the entity (77 provinces), β_0 the intercept coefficient, β_1 the slope coefficient, ρ the spatial lag parameter (*i.e.* the spatial correlation coefficient), W_{ij} the spatial weight matrix, and ε_i an error term that is normally distributed. Notably, the weight matrix (W_{ij}) of SLM defines the effects of neighbour j that influence location i (Anselin and Arribas-Bel, 2013; Mollalo *et al.,* 2020).

SEM assumes spatial dependence in the residuals, which are conventionally ignored in the ordinary least squares (OLS) model (Guo *et al.,* 2020; Wu *et al.*, 2020; Mollalo *et al.,* 2020). In particular, the residuals are decomposed into two components, u_i and ε_i, and spatially connected via the spatial correlation coefficient and the spatial weight matrix (W_{ij}).

SEM can be mathematically defined as follows:

$$\Delta logNTL_i = \beta_0 + \beta_1 logCOVID19_i + u_i, \qquad (4)$$

where u_i and u_j denote the disturbance term at locations i and j, respectively; λ the spatial correlation coefficient; ε_i an error term that is normally distributed; and $u_i = \lambda W_{ij} u_j + \varepsilon_i$.

Given that an ordinary least squares model (*i.e.* OLS regression) has a limitation in detecting the spillover effect, the standard specification is modified to incorporate the effects of neighbouring areas, leading to the formulation of SLM and SEM. SLM is based on a spatially lagged dependent variable and assumes the direct spatial influence between a particular area and the surrounding ones (Wu *et al.,* 2020). Meanwhile, SEM incorporates indirect spatial dependency into the regression model by allowing the influence of neighbouring areas to pass through the disturbance term (Anselin, 2003; Ward and Gleditsch, 2018; Mollalo *et al.,* 2020; Wu *et al.,* 2020).

Results

The monthly official statistics of COVID-19 infected cases are presented in Figure 2. The COVID-19 confirmed cases were 22,689 and 1,260,258 in the first and second major waves, respectively. Owing to the different variants of the COVID-19 virus, the number of infected cases in the second wave was much larger than that in the first one.

Local indicators of spatial association analysis

Figures 3-5 show the cluster analysis by using univariate LISA of the logarithm-transformed COVID-19 incidence rates of both major waves. In the first, the provinces with the statistically significant high rates were in the central region, namely, Samut Prakan province, and also located in the southern zone near the Malaysia border. In the second, the clusters of high incidence rates were observed in Bangkok, its vicinity and in the southern border

Figure 2. Monthly COVID-19 infected cases. *Source: Ministry of Public Health, Thailand.*
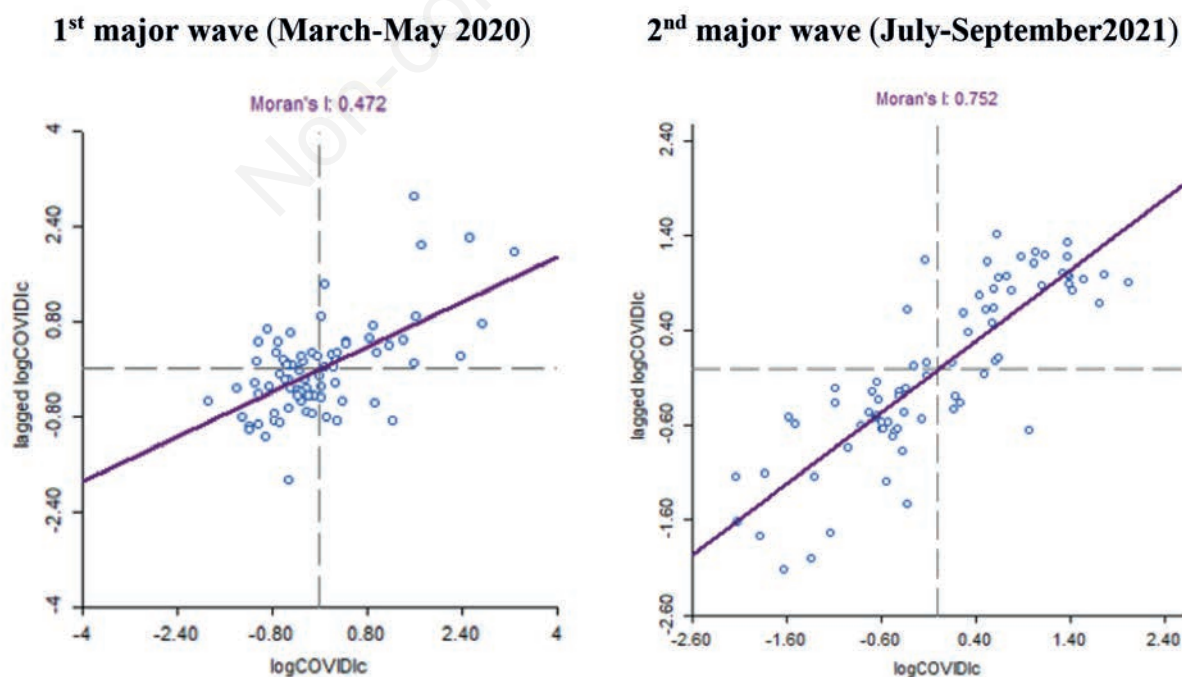

Figure 3. COVID-19 incidence (per 100,000 population). *Univariate LISA results.*
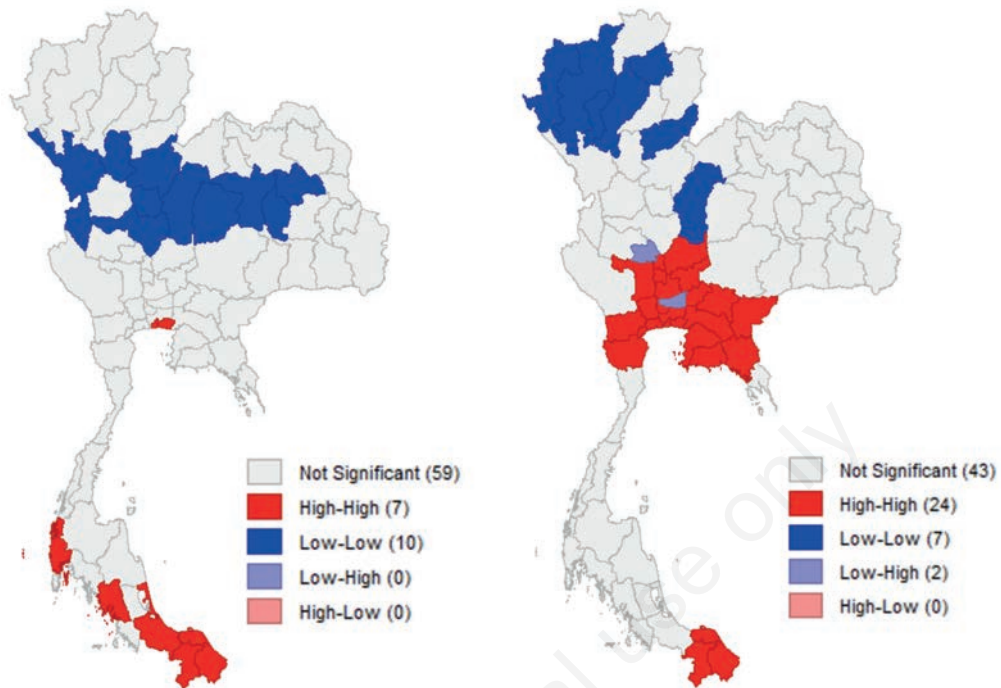
Figure 4. Cluster maps of COVID-19 incidence (per 100,000 population). *Univariate LISA results.*
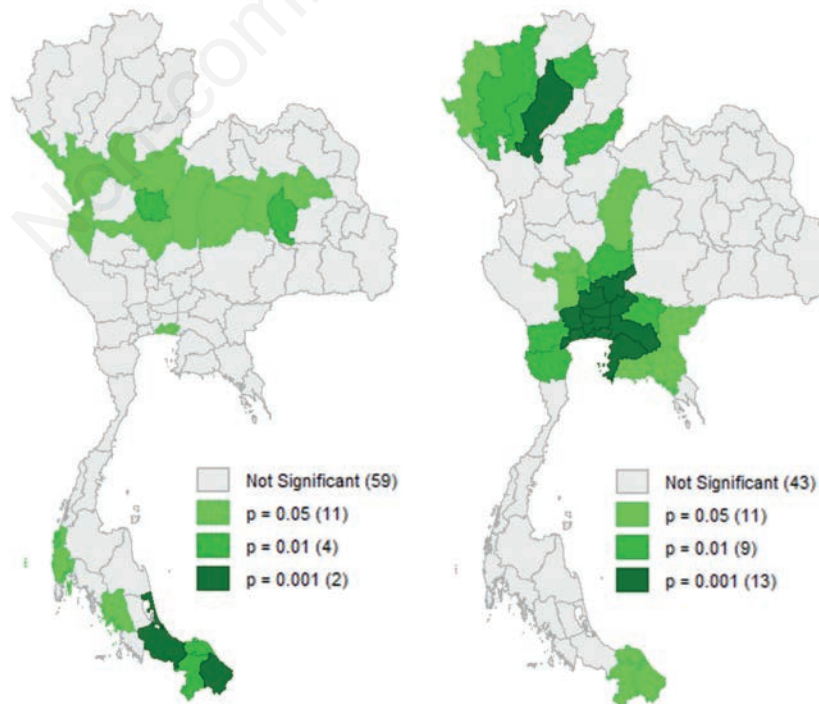
Figure 5. COVID-19 incidence (per 100,000 population): distribution of statistical significance. *Univariate LISA results.*

provinces. In both major waves, the clusters of statistically significant low rates were in several provinces in the northern region.

The outcomes of the bivariate LISA revealed the statistically significant negative correlation between the year-on-year change in logarithm-transformed NTL index and the logarithm of COVID-19 incidence rate in both waves. The LISA results are illustrated in Figures 6-8. All Moran's *I* values of the first and second waves were negative. The cluster maps of the two waves revealed the provinces that had a localised negative association between NTL density and the COVID-19 pandemic. In the first major wave, several southern provinces located near the Malaysia border and those located in the central region had a significant negative association between NTL density and COVID-19 incidence rate. In the second major wave, a similar relationship was found in the central region, particularly in Bangkok and vicinity, and also in the eastern coastal zone.

Regression analysis

The spatial modelling results are summarised in Table 1. For both major waves of the pandemic, the obtained slope coefficients of all regression models indicated that the growth of NTL density had a statistically significant negative association with the COVID-19 incidence rate ($P < 0.10$). The values of R^2 obtained from SLM and SEM explained approximately 50.73% and 50.74% of the variation in COVID-19 incidence rate in the first wave, respectively. In the case of the second wave, the corresponding values were 19.85% and 19.59%, respectively. The spillover spatial correlation coefficients of both SLM (λ) and SEM (ρ) also identified the statistically significant feature of localised spillover and specifically captured the spatial correlation effect of the dependent variable. This specification allows the slope coefficient (β_1) to accurately represent the relationship between NTL density and the outbreak of the COVID-19 pandemic.

Discussion

The official statistics showed a total of 1,282,947 confirmed cases of COVID-19 during the two major waves. As shown in Figure 2, the total number of infected cases during the second wave (July 2021-September 2021) was 1,259,407, whereas that during the first wave was only 3017. For both major waves, univariate and bivariate LISA analyses statistically detected the clusters of the COVID-19 pandemic and the localised negative associations between NTL and COVID-19 incidence rate. Furthermore, SLM and SEM regression methods verified a statistically significant relationship between NTL and the rate of COVID-19 infected cases.

Initially, the Thai government received many international accolades for its effective containment of COVID-19, that is based on the well-established infrastructure of the Universal Healthcare System (ADB, 2021). However, a combination of factors triggered the second wave and placed an extreme burden on the national healthcare system due to the overwhelming numbers of infected cases. Thus, as shown in Figure 2, the containment success during the first wave did not imply a similar, consistent capability in the subsequent phases of the pandemic, which was similar to other Asian economies, such as Vietnam and Taiwan (Khan and Javaid, 2020; Shams *et al.*, 2020; World Bank, 2021; Guo, 2020).

In addition, the outbreak of the COVID-19 pandemic is multifaceted. A spatial analysis was applied to the official data to examine the infected cases in spatiotemporal dimensions. As depicted in Figures 3-5, the spatial distributions of both major waves indicate that the highest incidence rate included clusters in the central provinces, the areas in Thailand with the highest population density. The clusters were also concentrated in several southern provinces located near the borders, which have a high concentration of cross-border activities and many immigrant workers.
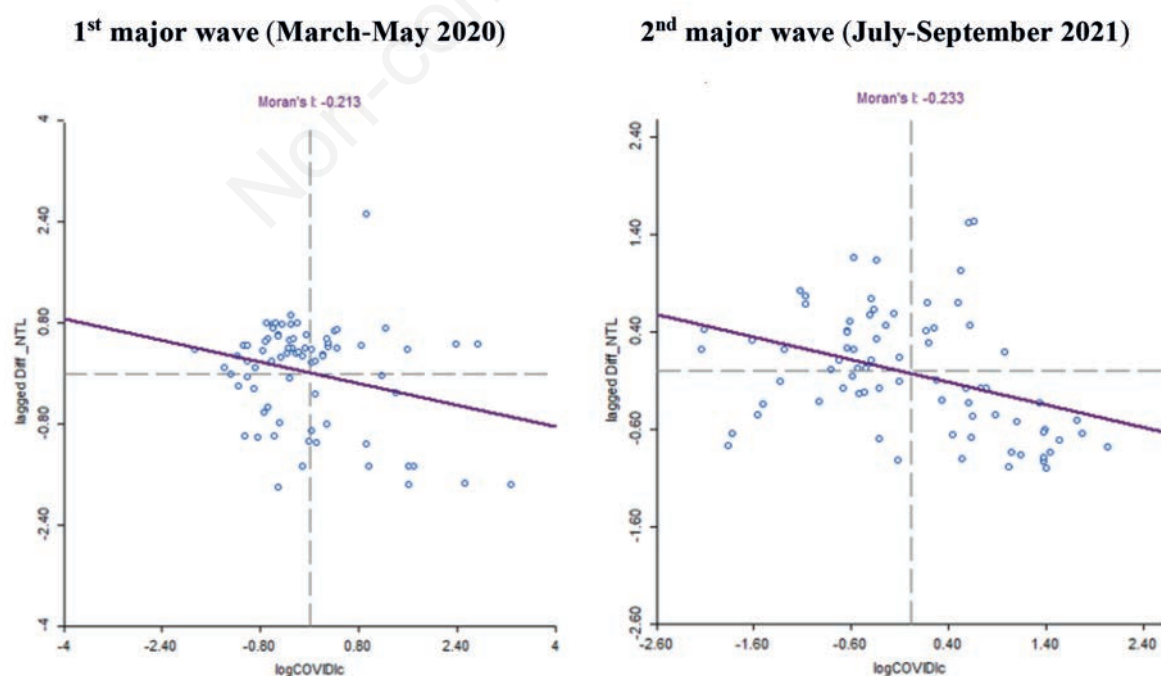

Figure 6. COVID-19 incidence rate and year-on-year nighttime light (NTL) change. *Bivariate LISA results.*
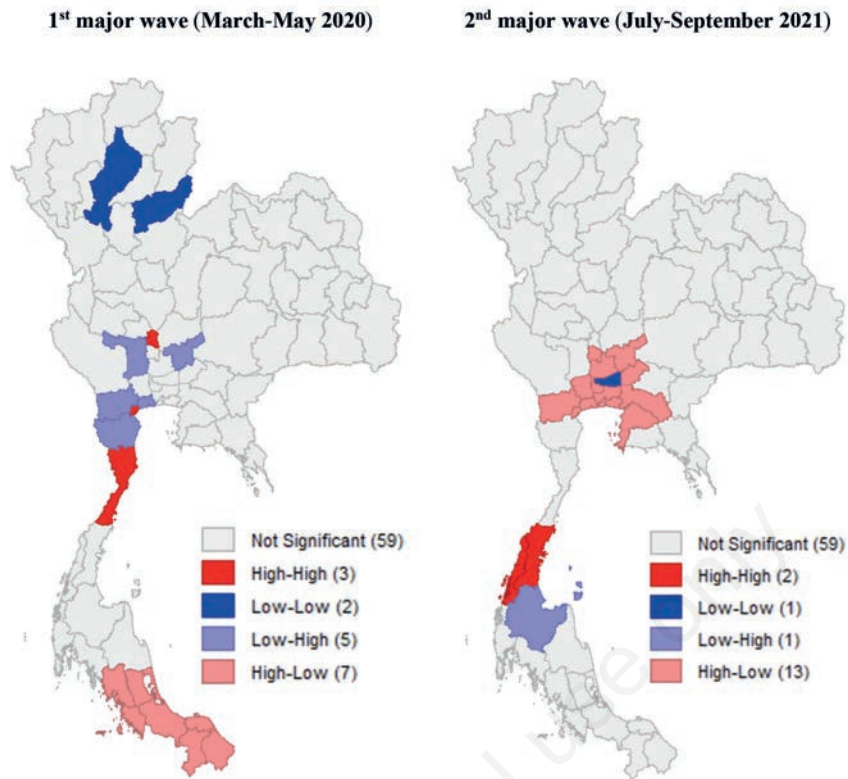
Figure 7. Cluster maps of COVID-19 incidence rate and year-on-year nighttime light (NTL) change. *Bivariate LISA results.*
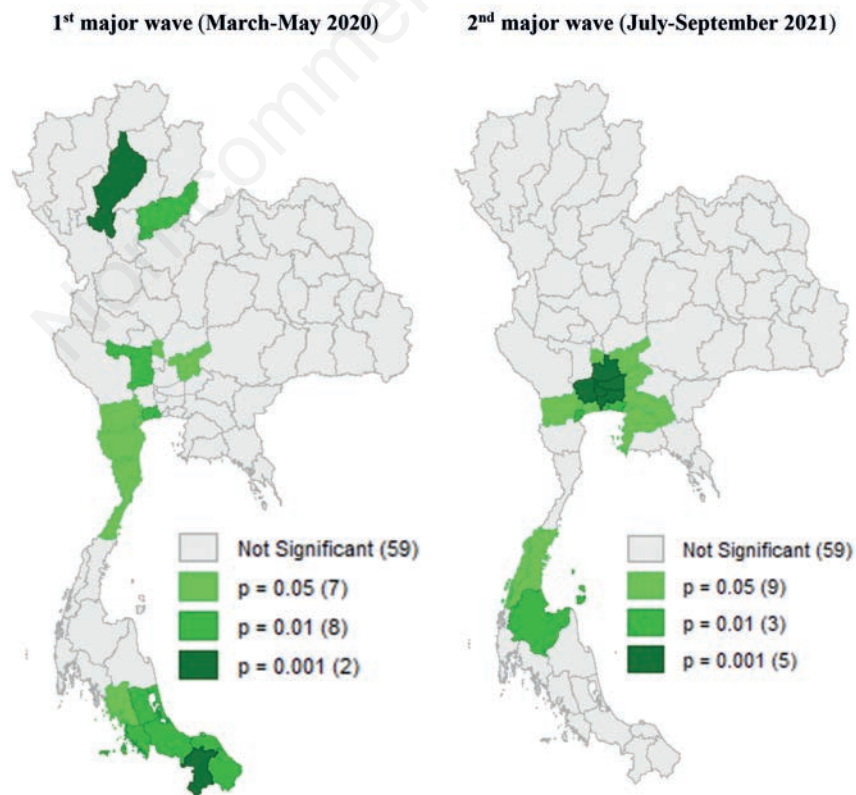

Figure 8. COVID-19 incidence rate and year-on-year nighttime light (NTL) change: distribution of statistical significance. *Bivariate LISA results.*

Meanwhile, in both waves, the clusters of low incidence were identified in the northern provinces, the region with the low population density due to its mountainous terrain. These patterns clearly indicate the association between the COVID-19 incidence rate and population density. In accordance with the experience of many countries, a similar association was found in Lebanon (El Deeb, 2021), Mainland China (Ning *et al.*, 2021), Turkey (Aral and Bakir, 2022), Oman (Al-Kindi *et al.*, 2020), and Bangladesh (Islam *et al.*, 2021). However, this association is inconclusive in several areas, such as São Paulo State of Brazil (Alcântara *et al.*, 2020).

The high rate of COVID-19 infected cases has led to reduced economic transactions and social activities. The NTL index, conventionally acknowledged as an alternative proxy of socioeconomic condition, can serve as a timely indicator of the concentration of mobility and transaction (Henderson *et al.*, 2012; Pinkovskiy and Sala-i-Martin, 2016; Li *et al.*, 2016). With the growing demand for publicly accessible alternative indicators providing timely information, the NTL index can potentially identify spatial clusters of the COVID-19 pandemic. The areas with high numbers of infected cases face either low growth or an adverse change in the NTL index.

During the outbreaks of the pandemic in Thailand, when restrictions were uniformly imposed across the country, the provinces with high rates of COVID-19 infections encountered significant declines in NTL density. Simultaneously, the restriction and containment policies influenced voluntary behavioural changes when the risks of infection increased (Maloney and Taskin, 2020; Abulibdeh, 2021). As exhibited in Figures 6-8, the bivariate LISA results statistically validated such negative association in several central and southern provinces. Similarly, Lan *et al.* (2021) suggested that a variation in NTL density is not only statistically correlated with the COVID-19 incidence rate, but it also extensively reflects the changes in human activity and the intensity of epidemic prevention and control measures in a particular region. Hence, Beyer *et al.* (2021) suggested NTL as the index for tracking and estimating the impact of COVID-19 outbreaks.

To extend the capability of impact estimation, the relationship between NTL density and COVID-19 infected cases can alternatively be examined by using regression analysis. As seen in Table 1, the results affirm the robustness of the statistically significant negative association between NTL growth and COVID-19 incidence rate (P-value<0.10). Similar to the findings of Jechow and Holker (2020), Elvidge *et al.* (2020), Beyer *et al.*, (2021), Small

and Sousa (2021) and Xu *et al.* (2021), the current study's results show that the NTL index can be a proxy for observing and approximating the socioeconomic impacts of the COVID-19 pandemic in the case of Thailand. However, the obtained values of R^2 shown in Table 1 remain insufficient to generate a highly accurate prediction, especially for estimating the impacts on monetary units. To enhance the predictive power, the forecasting model should incorporate additional specifications and other alternative high-frequency data, such as mobility index, electricity and water consumption, and mobile phone utilisation (Demirguc-Kunt *et al.*, 2020; Li *et al.*, 2020; Ruan *et al.*, 2020; Bustamante-Calabria *et al.*, 2021).

Conclusions

An association between COVID-19 incidence rate and NTL growth during the pandemic was confirmed, especially in Bangkok, the central region and the southern border provinces. Thus, the localised effects of the COVID-19 outbreak can be timely identified using the NTL index. For future improvements, an extension that incorporates additional variables into the regression models can be a method for precisely estimating the socioeconomic impacts of the COVID-19 pandemic.

References

Abulibdeh A, 2021. Modeling electricity consumption patterns during the COVID-19 pandemic across six socioeconomic sectors in the State of Qatar. Energy Strategy Rev 38:1-17.

Alcântara E, Mantovani J, Rotta L, Park E, Rodrigues T, 2020. Investigating spatiotemporal patterns of the COVID-19 in São Paulo State, Brazil. Geospat Health 15:201-9.

Al-Kindi KM, Alkharusi A, Alshukaili D, 2020. Spatiotemporal assessment of COVID-19 spread over Oman using GIS techniques. Earth Syst Environ 4:797-811.

Ahasan R, Hossain MM, 2021. Leveraging GIS and spatial analysis for informed decision-making in COVID-19 pandemic. HPT 10:7-9.

Anselin L, 1995. Local indicators of spatial association (LISA). Geogr Anal 27:93-115.

Anselin L, 2003. An introduction to spatial autocorrelation analy-

Table 1. Estimated parameters obtained from spatial lag model and spatial error model models.

	First major wave		Second major wave	
	SLM	**SEM**	**SLM**	**SEM**
Constant	0.0153 (P=<0.001)	0.0374 (P=<0.001)	0.0216 (P=0.042)	0.0284 (P=0.038)
Log COVID19	−0.0078 (P=<0.001)	−0.0086 (P=0.067)	−0.0064 (P=0.056)	−0.0083 (P=0.056)
ρ	0.6245 (P=<0.001)	-	0.3615 (P=0.020)	-
λ	-	0.6416 (P=<0.001)	-	0.3623 (P=0.023)
R-squared	0.5073	0.5073	0.1985	0.1959
Observations	77	77	77	77

P-value=0.10 is a threshold level of statistical significance. Dependent variable: $\Delta logNTL$ [the year-on-year change in the logarithm-transformed NTL (nighttime light) index]. SLM spatial lag model; SEM, the spatial error model.

sis with GeoDa. Spatial Analysis Laboratory, University of Illinois, IL, USA. Available from: https://personal.utdallas.edu/~briggs/poec6382/geoda_spauto.pdf

Anselin L, Syabri I, Kho Y, 2006. GeoDa: an introduction to spatial data analysis. Geogr Anal 38:5-22.

Anselin L, Arribas-Bel D, 2013. Spatial fixed effects and spatial dependence in a single cross-section. Pap Reg Sci 92:3-17.

Aral N, Bakir H, 2022. Spatiotemporal analysis of Covid-19 in Turkey. Sustain Cities Soc 76:103421.

Asian Development Bank (ADB), 2021. Pandemic preparedness and response strategies: COVID-19 lessons from the Republic of Korea, Thailand, and Viet Nam. Available from: https://www.adb.org/sites/default/files/publication/743746/pandemic-preparedness-covid-19-lessons.pdf

Bergquist R, Rinaldi L, 2020. Covid-19: Pandemonium in our time. Geospat Health 15:1-5.

BeyerRC, Franco-BedoyaS, Galdo V, 2021. Examining the economic impact of COVID-19 in India through daily electricity consumption and nighttime light intensity. World Dev 140:1-33.

Bustamante-Calabria M, Sánchez de Miguel A, Martín-Ruiz S, Ortiz J L, Vílchez JM, 2021. Effects of the COVID-19 lockdown on urban light emissions: ground and satellite comparison. Remote Sens 13:1-21.

Cao C, Chang C, Xu M, Zhao J, Gao M, et al., 2010. Epidemic risk analysis after the Wenchuan Earthquake using remote sensing. Int J Remote Sens 31:3631-42.

Demirgüç-Kunt A, Lokshin M, Torre I, 2020. The sooner, the better: The early economic impact of non-pharmaceutical interventions during the COVID-19 pandemic. World Bank Policy Res Work Pap 9257:1-93.

Department of Disease Control (DDC), 2021. Thailand Situation (COVID-19). Department of Disease Control, Nonthaburi, Thailand. Available from: https://covid19.ddc.moph.go.th/

El Deeb O, 2021. Spatial autocorrelation and the dynamics of the mean centre of COVID-19 infections in Lebanon. Front Appl Math Stat 6:620064.

Elvidge CD, Ghosh T, Hsu FC, Zhizhin M, Bazilian M, 2020. The dimming of lights in China during the COVID-19 pandemic. Remote Sens 12:1-16.

Fatima M, O'Keefe KJ, Wei W, Arshad S, Gruebner O, 2021. Geospatial Analysis of COVID-19: A Scoping Review. Int J Environ Res Public Health 18:2-14.

Grainger R, Machado PM, Robinson PC, 2021. Novel coronavirus disease-2019 (COVID-19) in people with rheumatic disease: epidemiology and outcomes. Best Pract Res Clin Rheumatol 101657:1-11.

Guo A, Yang J, Xiao X, Xia J, Jin C, 2020. Influences of urban spatial form on urban heat island effects at the community level in China. Sustain. Cities Soc 53:101972.

Henderson JV, Storeygard A, Weil DN, 2012. Measuring economic growth from outer space. Am Econ Rev 102:994-1028.

Iftimie S, López-Azcona AF, Vallverdú I, Hernández-Flix S, De Febrer G, 2021. First and second waves of coronavirus disease-19: A comparative study in hospitalised patients in Reus, Spain. PLoS One 16:1-13.

Islam A, Sayeed MA, Rahman MK, Ferdous J, Islam S, Hassan MM, 2021. Geospatial dynamics of COVID-19 clusters and hotspots in Bangladesh. Transbound Emerg Dis 68:3643-57.

Jechow A, Hölker F, 2020. Evidence that reduced air and road traffic decreased artificial night-time skyglow during COVID-19 lockdown in Berlin, Germany. Remote Sens 12:1-23.

Khan A, Haleem, Javaid M, 2020. Analysing COVID-19 pandemic through cases, deaths, and recoveries. JOBCR10:450-69.

Kolak M, Li X, Lin Q, Wang R, Menghaney M, et al., 2021. The US COVID Atlas: A dynamic cyberinfrastructure surveillance system for interactive exploration of the pandemic. Trans GIS 25:1741-65.

Kraemer MU, Yang CH, Gutierrez B, Wu CH, Klein B, et al., 2020. The effect of human mobility and control measures on the COVID-19 epidemic in China. Sci 368:493-97.

Kunno J, Supawattanabodee B, Sumanasrethakul C, Wiriyasivaj B, Kuratong S, 2021. Comparison of different waves during the COVID-19 pandemic: retrospective descriptive study in Thailand. Adv Prev Med 2021:1-8.

Lan T, Shao G, Tang L, Xu Z, Zhu W, 2021. Quantifying spatiotemporal changes in human activities induced by COVID-19 pandemic using daily nighttime light data. IEEE J Sel Top Appl Earth Obs Remote Sens 14:2740-53.

Liu Q, Li Y, Yu M, Chiu LS, Hao X, 2019. Daytime rainy cloud detection and convective precipitation delineation based on a deep neural network method using GOES-16 ABI images. Remote Sens 11:1-18.

Liu Q, Sha D, Liu W, Houser P, Zhang L, 2020. Spatiotemporal patterns of COVID-19 impact on human activities and environment in mainland China using nighttime light and air quality data. Remote Sens 12:1-14.

Li D, Zhao X, Li X, 2016. Remote sensing of human beings–a perspective from nighttime light. Geo Spat Inf Sci 19:69-79.

Li K, Liang Y, Li J, Liu M, Feng Y, 2020. Internet search data could Be used as novel indicator for assessing COVID-19 epidemic. Infect Dis Model 5:848-54.

Luenam A, Puttanapong N, 2020. Modelling and analyzing spatial clusters of leptospirosis based on satellite-generated measurements of environmental factors in Thailand during 2013-2015. Geospat Health 15:217-24.

Maloney WF, Taskin T, 2020. Determinants of social distancing and economic activity during COVID-19: A global view. World Bank Policy Res Work Pap 9242:1-21.

Mollalo A, Vahedi B, Rivera KM, 2020. GIS-based spatial modeling of COVID-19 incidence rate in the continental United States. Sci Total Environ 728:1-8.

Moran PAP, 1950. Notes on continuous stochastic phenomena. Biometrika 37:17-23.

Ministry of Public Health (MoPH), 2021. Strategy: Managing the new wave of the Covid-19 epidemic. Ministry of Public Health. Nonthaburi. Thailand. Available from: https://ddc.moph.go.th/viralpneumonia/eng/file/main/en_Thailand%20Covid-19%20plan_MOPH_2021.pdf

National Oceanic and Atmospheric Administration (NOAA), 2019. National Centers for Environmental Information. Version 1 VIIRS day/night band nighttime lights. Available from: https://www.ngdc.noaa.gov/eog/viirs/download_dnb_composites.html

Ning J, Chu Y, Liu X, Zhang D, Zhang J, et al., 2021. Spatio-temporal characteristics and control strategies in the early period of COVID-19 spread: a case study of the mainland China. Environ Sci Pollut Res Int 28:48298-311.

Pinkovskiy M, Sala-i-Martin X, 2016. Lights, camera…income! Illuminating the national accounts-household surveys debate. Q J Econ 131:579-631.

Puttanapong N, Martinez Jr. A, Addawe M, Bulan JAN, Durante

RL, 2020. Predicting poverty using geospatial data in Thailand. Asian Development Bank Economics Working Paper Series No. 630. Available from: https://www.adb.org/publications/predicting-poverty-using-geospatial-data-thailand

Ruan G, Wu D, Zheng X, Zhong H, Kang C, 2020. A cross-domain approach to analyzing the short-run impact of COVID-19 on the US electricity sector. Joule 4:2322-37.

Sangkasem K, Puttanapong N, 2021. Analysis of spatial inequality using DMSP-OLS nighttime-light satellite imageries: a case study of Thailand. Reg Sci Policy Pract 1-22.

Shams SA, Haleem A, Javaid, M, 2020. Analyzing COVID-19 pandemic for unequal distribution of tests, identified cases, deaths, and fatality rates in the top 18 countries. Diabetes Metab Syndr Clin Res Rev 14:953-61.

Small C, Sousa D, 2021. Spatiotemporal evolution of COVID-19 infection and detection within night light networks: comparative analysis of USA and China: Appl Netw Sci 6:10.

Sun F, Matthews SA, Yang TC, Hu MH, 2020. A spatial analysis of the COVID-19 period prevalence in US counties through June 28, 2020: where geography matters?. Ann Epidemiol 52:54-9.

Steiniger S, Hunter AJ, 2013. The 2012 free and open source GIS software map: A guide to facilitate research, development, and adoption. Comput Environ Urban Syst 39:136-50.

Ward MD, Gleditsch KS, 2018. Spatial regression models. Sage Publications.

WHO, 2020. WHO Thailand situation report - 1. Available from: https://cdn.who.int/media/docs/default-source/searo/ thailand/20200206-tha-sitrep-01-ncov-final.pdf?sfvrsn= 7c8cb671_0

WHO, 2021. WHO Thailand situation report - 203. Available from: https://cdn.who.int/media/docs/default-source/searo/ thailand/2021_09_30_eng-sitrep-203-covid19.pdf?sfvrsn=97 de5f7b_5

WHO, 2022. Coronavirus disease (COVID-19) Weekly Epidemiological Update and Weekly Operational Update. Available from: https://www.who.int/emergencies/ diseases/ novel-coronavirus-2019/situation-reports

World Bank, 2021.A year deferred - early experiences and lessons from Covid-19 in Vietnam. Available from: http://documents.worldbank.org/curated/en/826921633442977133/A-Year-Deferred-Early-Experiences-and-Lessons-from-Covid-19-in-Vietnam

Wu Z, Chen Y, Han Y, Ke T, Liu Y, 2020. Identifying the influencing factors controlling the spatial variation of heavy metals in suburban soil using spatial regression models. Sci Total Environ 717:137212.

Xu H, Yu T, Gu XF, Cheng TH, Xie DH, et al., 2013. The research on remote sensing dust aerosol by using split window emissivity. Spectrosc Spect Anal 33:1189-93.

Xu G, Xiu T, Li X, Liang X, Jiao L, 2021. Lockdown induced night-time light dynamics during the COVID-19 epidemic in global megacities. Int J Appl Earth Obs 102:102421.